Articles

High-Surface-Area Nanocrystalline Cerium Phosphate through Aqueous Sol−Gel Route

K. Rajesh,† P. Mukundan,† P. Krishna Pillai,† V. R. Nair,‡ and K. G. K. Warrier†,*

Ceramic Technology Division, Regional Research Laboratory, Council of Scientific & Industrial Research, Thiruvananthapuram 695 019, India, and Indian Rare Earths Ltd., Udyogamandal, Alwaye 683 501, India

Received January 15, 2004. Revised Manuscript Received March 29, 2004

Rare earth phosphates have recently been investigated as a potential ceramic material in view of their high-temperature phase stability, high melting point, low thermal conductivity, optical, fluorescence, and catalytic properties, and layered structural features. The present work describes a method for synthesizing nanocrystalline cerium phosphate starting from cerium nitrate and orthophosphoric acid by sol−gel process involving controlled precipitation followed by electrostatic stabilization (peptization) using nitric acid and deagglomeration of sol particles using ultrasonication. Average particle size of cerium phosphate in the precursor sol is 50 nm. Dehydroxylation of the precursor gel was studied by thermal analysis and FTIR spectrum. The transformation of low-temperature rhabdophane phase to hexagonal and further to monoclinic monazite type at 800 °C is evidenced from the XRD pattern. Cerium phosphate had crystallite size of 10 nm and excellent thermal phase stability up to 1700 °C as observed from XRD data. Specific surface area of 98 m^2/g was obtained for precursor gel calcined at 400 °C. The nanosize cerium phosphate has been sintered at 1300 °C to ∼99% density with an average grain size of 1 μm as observed from SEM micrographs.

Introduction

The family of rare earth phosphates was shown to possess excellent thermal phase stability and high melting point above 1900 °C[1] and this generated considerable interest in the synthesis of fine-grained compositions and evaluation of properties such as densification characteristics, thermal conductivity, reactivity with other ceramic oxides, catalytic and optical properties,[2] and suitability as second phase in ceramic matrix composites. Lanthanum phosphate is reported widely in the literature. Morgan et al. found that lanthanum phosphate has no reactivity with alumina, but has a nearly identical thermal expansion coefficient.[3] Lanthanum phosphate−alumina composite was shown to have machinable characteristics like that of micor but had better thermal stability.[4] The melting point of synthetic cerium phosphate was first reported by Hikichi to be 2045 ± 20 °C and was synthesized by conventional precipitation technique.[1] Composites of zirconia and alumina containing cerium phosphate as second phase particles are also reported.[5] Cerium and lanthanum phosphate were used as catalysts for oxidative dehydrogenation of isobutane to isobutene and vapor-phase O-alkylation of phenol over alkali.[6,7] Further, catalytic efficiency of such phosphates on dehydration reaction of 2-propanol, cracking/dehydrogenation reaction of cumene, and isomerization reaction of butene were studied by Onoda et al.[8]

Hikichi et al. prepared monazite-type $CePO_4$ by heating $CePO_4 \cdot 0.5H_2O$ and reported a high sintered density (99%) at 1500 °C.[9] Another approach to synthesize cerium phosphate was through the reaction between rare earth salts and ammonium phosphate.[10] $CePO_4$ was prepared from $Ce_2(SO_4)_3 \cdot H_2O$ using $NH_2H_2PO_4$ solution as a reagent and used for thermophysical property measurement and ion implantation studies.[11] Recently, a mechanochemical method has also been used to synthesize rhabdophane-type $CePO_4$ by

* Corresponding author. Fax: +91-471-2491712. Tel: +91-471-2515227. E-mail: warrierkgk@yahoo.com or warrier@csrrltrd.ren.nic.in.
† Council of Scientific Industrial Research.
‡ Indian Rare Earths Ltd.

(1) Hikichi, Y.; Nomura, T. *J. Am. Ceram. Soc.* **1987**, *70*, (10), C-252.
(2) (a) Riwotzaki, K.; Meyssamy, H.; Kornowski, A.; Haase, M. *J. Phys. Chem. B.* **2000**, *104*, 2824. (b) Meyssamy, H.; Riwotzaki, K.; Kornowski, A.; Naused, S.; Haase, M. *Adv. Mater.* **1999**, *11* (10), 840. (c) Riwotzki, K.; Meyssamy, H.; Schnablegger, H.; Kornowski, A.; Haase, M. *Angew. Chem., Int. Ed.* **2001**, *40*, 3. (d) Rambabu, V.; Buddhudu, S. *Opt. Mater.* **2001**, *17*, 401. (e) Yu, M.; Lin, J.; Fu, J.; Han, Y. C. *Chem. Phys. Lett.* **2003**, *371*, 178.
(3) Morgan, P. E. D.; Marshall, D. B. *J. Am. Ceram. Soc.* **1995**, *78* (6), 1553.
(4) Morgan, P. E. D.; Marshall, D. B. R.; Housley, M. *Mater. Sci. Eng. A.* **1995**, *195*, 215. (b) Min, W.; Miyahara, D.; Yokoi, K.; Daimon, K.; Matsuan, T.; Hikichi, Y. *Mater. Res. Bull.* **2002**, *37*, 1107.
(5) (a) Davis, J. B.; Marshall, D. B.; Housley, R. M.; Morgan, P. E. D. *J. Am. Ceram. Soc.* **1998**, *81* (8), 2169. (b) Gao, H.; Liu, H. C.; Du, H. Y. *Scr. Mater.* **2003**, *49* (6), 515.
(6) Takita, Y.; Sano, K.; Muraya, T.; Nishiguchi, H.; Kawata, N.; Ito, M.; Ishihara, T. *Appl. Catal. A: Gen.* **1998**, *170*, 23.
(7) Sarala Devi, G.; Giridhar, D.; Reddy, B. M. *J. Mol. Catal. A: Chem.* **2002**, *181*, 173.
(8) Onoda, H.; Nariai, H.; Moriwaki, A.; Motooka, I. *J. Mater. Chem.* **2002**, *12*, 1754.
(9) Hikichi, Y.; Nomura, T.; Tanimura, Y.; Suzuski, S.; Miyami, M. *J. Am. Ceram. Soc.* **1990**, *73* (12), 3594.

10.1021/cm0499139 CCC: $27.50
Published on Web 06/09/2004

grinding $Ce(NO_3)_3 \cdot 6H_2O$, $CeCl_3 \cdot 7H_2O$, and $Ce_2(CO_3) \cdot 8H_2O$ along with $(NH_4)_2HPO_4$.[12] Cerium phosphate was prepared by reaction with cerium nitrate and phosphoric acid[13] and also by hydrolysis of cerium butoxide, which were used for coating on alumina fibers.[14] Synthesis of microcrystalline cerium phosphate, using cerium nitrate and phosphoric acid, in ethanolic media was reported by Yan Guo et al.[15] However, there is no literature available on synthesis of nanosize cerium phosphate by sol−gel process and involving electrostatic stabilization and gelation in ammonia atmosphere. For applications related to catalysis, coatings, and low-temperature densification, and for synthesis of nanocomposites, nanosize particle is very important. Therefore, we report a procedure for the preparation of monomodal nanosize cerium phosphate sol by controlled precipitation of cerium nitrate in aqueous solution, followed by electrostatic stabilization (peptization) by nitric acid, and further subjecting the sol to ultrasonication for a period of 15 min. The stable sol was then gelled by exposing it in an ammonia atmosphere for 2 days. The gel to cerium phosphate formation, particle characterization, thermal phase stability, high surface area, and low-temperature densification are presented.

Experimental Section

Cerium nitrate, 99.9% pure (M/s Indian Rare Earths Ltd. India) and orthophosphoric acid (AR grade, 88%, Qualigens Fine Chemicals, India) were used as starting materials. A 0.03 M (9.239 g) solution of $Ce(NO_3)_3 \cdot 6H_2O$ was prepared in deionized water. Orthophosphoric acid solution (2.084 g (1.191 mL)) was added slowly to the cerium nitrate solution while kept under stirring. An off-white precipitate of cerium phosphate was obtained. The precipitate was then filtered and washed free of nitrates and phosphates, and was further redispersed in deionized water. The electrostatic stabilization was achieved by addition of 20% nitric acid where the pH was adjusted in the range 1.8−2. The suspension was kept under stirring for about 4 h. The colloidal sol thus obtained was further subjected to ultrasonication for 15 min to obtain stable cerium phosphate precursor sol. Particle size distribution of the precursor sol and zeta potential were measured using laser light diffraction method (Zeta Sizer, Malvern Instruments Ltd., UK). Gelation of the sol was carried out by exposing it to ammonia atmosphere over a period of 48 h in a closed desiccator. Cerium phosphate gel thus obtained was dried at 80 °C. The preparation procedure is presented as a flow diagram in Figure 1. Thermal decomposition features of the precursor gel were studied in air at a heating rate of 10 °C/min using a Shimadzu Thermal Analyzer, Japan (model 50H). Densification and shrinkage features of cerium phosphate were recorded using a thermo mechanical analyzer (TMA) Shimadzu 60H (Japan), up to a temperature of 1350 °C on a cylindrical sample of 10-mm diameter and 8-mm length made by pressing the 400 °C calcined gel power. The rate of heating of 10 °C/min and air atmosphere were employed. The precursor gel was separately heated at various temperatures in the range 400−1700 °C, and phase identification was done by XRD (Philips PW 1710) on the calcined powders in the 2θ range 20−60° using Cu Kα radiation. The crystallite size was calculated by the X-ray line broadening method using the Scherrer equation

$$t = \frac{0.9\lambda}{\beta \cos\theta}$$

where t is the crystallite size, λ is the wavelength of radiation (1.54 Å for Cu Kα radiation), β is the corrected peak width at half-maximum intensity, and θ is angle of diffraction at the peak position. BET surface area and pore size distribution of the gel after calcination at 400 and 800 °C were measured by nitrogen adsorption (after degassing the powders at 200 °C for 4 h) using a Micromeritics Gemini 2375 V5.01 surface area analyzer. FT-IR spectra of cerium phosphate calcined at different temperatures were taken using a Nicolet Magna-IR 560 spectrophotometer as KBr pellets in the range of 400−4000 cm^{-1}. The calcined powder was compacted at pressure of 200 MPa to pellets (11 mm dia and 2 mm thick). The pellets were sintered in the range 1100−1400° C, at a heating rate of 10 °C/ min, and soaked at the peak temperature for 3 h. The relative density was measured by the Archemedes method. The polished, thermally etched surface of sintered cerium phosphate after providing gold coatings was observed under a scanning electron microscope (Hitachi, 2240 Japan). Cerium phosphate precursor gel, after being calcined at 400 °C, was observed under a transmission electron microscope (JEOL 3000EX, with an accelerating voltage of 300 keV) for its nanosize characteristics.

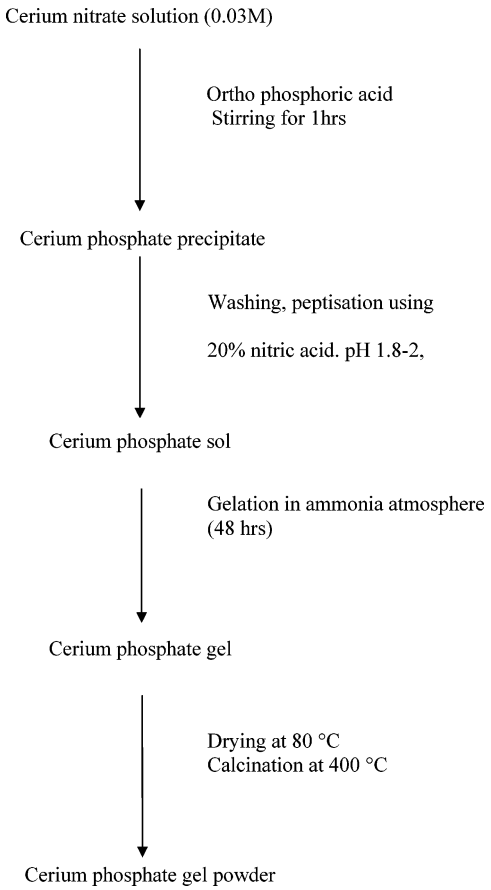

Figure 1. Flow diagram of the preparation of cerium phosphate nanoparticles.

Results and Discussion

In the present investigation the cerium phosphate precipitate was electrostatically stabilized to nanosize

(10) (a) Onoda, H.; Narini, H.; Maki, H.; Motooka, I. *Mater. Chem. Phys.* **2002**, *73*, 19. (b) Ruigang, W.; Wei, P.; Jain, C.; Minghao, F.; Zhenzhu, C.; Yongming, L. *Mater. Chem. Phys.* **2002**, *9666*, 1.

(11) (a) Bakker, K.; Hein, H.; Konings, R. J. M.; van der Laan, R. R.; Matzke, H.; van Vlaanderen, P. *J. Nucl. Mater.* **1998**, *252* (3), 228. (b) Meldrum, A.; Wang, L. M.; Ewing, R. C. *Nucl. Instrum. Methods Phys. Res., Sect. B* **1996**, *116* (1−4), 220.

(12) Onoda, H.; Nariai, H.; Maki, H.; Motooka, I. *Mater. Chem. Phys.* **2003**, *78* (2), 400.

(13) Bo, L.; Liya, S.; Xiaozhen, L.; Tianmain, W.; Ishii, K.; Sasaki, Y.; Kashiwaya, Y.; Takahashi, H.; Shibayama, T. *J. Mater. Sci. Lett.* **2000**, *19*, 343.

(14) Bo, L.; Liya, S.; Xiaozhen, L.; Shuiche, Z.; Yumeri, Z.; Tianmain, W.; Sasaki, Y.; Ishii, K.; Kashiwaya, Y.; Takahashi, H.; Shibayama, T. *J. Mater. Sci. Lett.* **2001**, *20*, 1071.

(15) Guo, Y.; Woznicki, P.; Barkatt, A. *J. Mater. Res.* **1996**, *11* (3), 639.

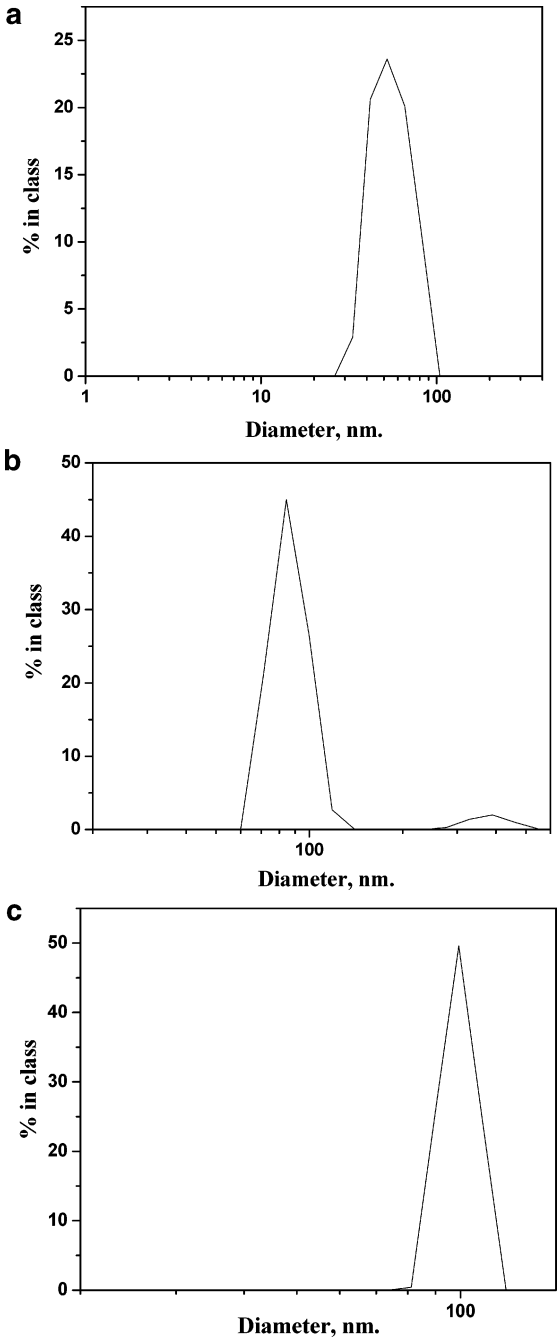

Figure 2. Particle size distribution of cerium phosphate precursor sol (a), precursor sol aged for one year (b), and one-year-aged sol after ultrasonication (c).

colloidal sol by controlling the zeta potential above 52 mV and by maintaining the pH in the range 1.8−2. At pH above 4, the stability of the sol is lost and gradual agglomeration sets in. The particle size distribution of cerium phosphate sol is presented in Figure 2a. The stable sol shows a monomodal distribution of cerium phosphate particles with an average size of about 50 nm. We could not observe any visible sedimentation or flocculation even after keeping the sol for a year. There was, however, a very slow tendency for the sol particles to undergo particle growth resulting in a bimodal distribution consisting of particles of size 86 and 380 nm (Figure 2b); i.e., after one year, about 95% of the particles were still in the size of 86 nm. When this sol was ultrasonicated for 15 min, cerium phosphate particles with an average particle size of 99 nm (Figure 2c)

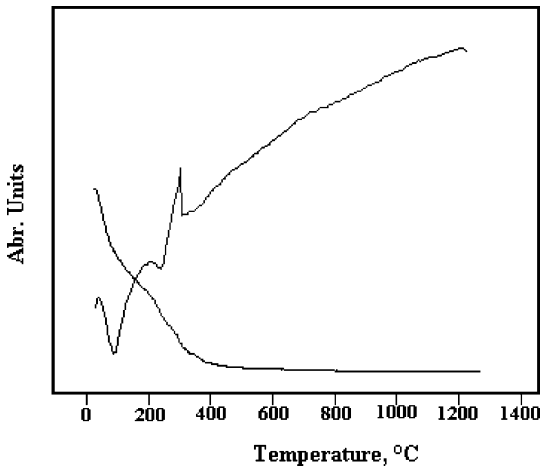

Figure 3. Thermal analysis (DTA/TGA) graph of cerium phosphate precursor gel.

were obtained. The zeta potential of this sol was 42 mV. This reduction in zeta potential from 52 to 42 mV may be due to the reduction in the effective charge density by decreasing the surface area as a result of the increased particle size. This increase in particle size could be attributed to a possible dissolution−reprecipitation process occurring in the sol, on the larger particle at the expense of smaller particles.[16]

Decomposition of the precursor gel and formation of cerium phosphate were followed by thermal analysis data provided in Figure 3. The TGA curve shows three-step decomposition of cerium phosphate precursor gel. The weight loss of 15% was observed below 450 °C. The first step weight loss between 28 and 110 °C corresponds to the removal of adsorbed water. The evolution of water of hydration of cerium phosphate takes place between 110 and 245 °C. This is about ∼1 mol of water per mol of cerium phosphate.

$$CePO_4 \cdot 1H_2O \rightarrow CePO_4 + 1H_2O$$

This is nearly identical to the evolution of water of hydration of monazite-type lanthanum phosphate reported by Boakye et al.[17] The third weight loss between 245 and 420 °C is attributed to loss of nitrate, which originates from the peptization step, where nitric acid was used as peptizing agent. Although nitric acid should vaporize well below 420 °C, the residual nitrate can easily be complexed and trapped in nanoporous precursor gel. A small weight loss of 0.682% between 420 and 800 °C may be attributed to this residual nitrate. A similar phenomenon was reported in lanthanum phosphate precursor by Boakye et al.[17a] DTA analysis shows two endothermic peaks at 91 and 235 °C corresponding to the loss of adsorbed water and water of hydration, respectively. An intense exothermic peak at 303 °C corresponds to evolution of nitrates. A weak exothermic peak at 730 °C may be due to the crystallization of monazite-type $CePO_4$ from hexagonal form.[13,14]

The FTIR spectra taken on the precursor gel, as well as after calcination, at different temperatures are presented in Figure 4a and b. The peak around 3500 cm^{-1} of the precursor gel is due to −OH stretch and the

(16) Klein, S. M.; Choi, J. H.; Pine, D. J.; Lange, F. F. *J. Mater. Res.* **2003**, *18* (6), 1457.

(17) (a) Boakye, E. E.; Hay, R. S.; Mogilevsky, P.; Douglas, L. M. *J. Am. Ceram. Soc.* **2001**, *84* (12), 2793. (b) Boakye, E. E.; Hay, R. S.; Petry, M. *J. Am. Ceram. Soc.* **1999**, *82* (9), 2321.

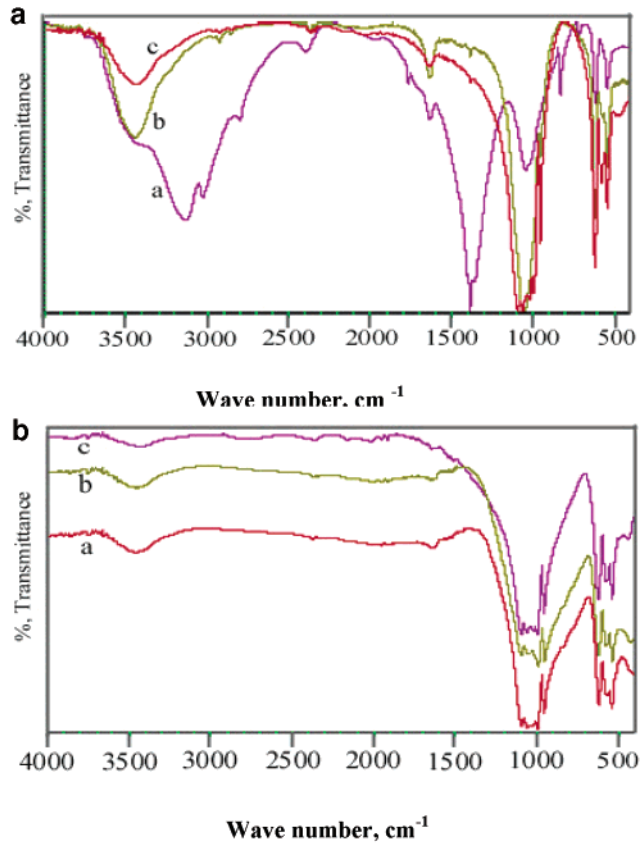

Figure 4. (a) FTIR spectra of cerium phosphate heated at 80 (trace a), 400 (trace b), and 800 °C (trace c); and (b) heated at 1000 (trace a), 1300 (trace b), and 1700 °C (trace c).

peak around 1600 cm^{-1} is attributed to −OH bending mode. FTIR spectra of the gel sample dried at 80 °C show a broad and large peak with some shoulders between 3000 and 3500 cm^{-1}. This may be due to the change in the OH environments in gel stage, like hydrogen bonding in the presence of ammonia. The intensity of these peaks decreases along with temperature. Vibrational spectra of hydrated rare earth orthophosphates, i.e., rhabdophane and weinschenkite-type, were examined by Assaaoudi et al. and a peak at 750 cm^{-1} is assigned as rocking modes involving water molecules.[18] A peak appearing in this work at 715 cm^{-1} for cerium phosphate dried at 80 °C may be assigned to the rocking mode of vibrations of water molecule. The peaks at 1380 and 878 cm^{-1} corresponded to nitrate group and are more prominent than phosphate P−O stretching in gel dried at 80 °C. But the P−O absorption at 1040 cm^{-1} is prominent in gel heated at 400 °C. A weak band of the complexed or trapped residual nitrate at 1380 cm^{-1} spectra of cerium phosphate gel calcined at 800 °C was observed, and this supports the thermal analysis data. At higher temperatures the nitrate groups are absent. The P−O stretching peak is single and broad in cerium phosphate calcined at 400 °C, but above 800 °C the P−O stretching appears as split bands. This may be due to the dehydration in the gel giving flexibility to phosphate bonds. All the spectra taken on phosphate gel heated above 800 °C showed similar characteristic peaks. Peaks around 1040, 616, and 540 cm^{-1} correspond to P−O stretching, O=P−O bending,

(18) Assaaoudi, H.; Ennaciri, A.; Rulmoat, A. *Vib. Spectrosc.* **2001**, *25*, 81.

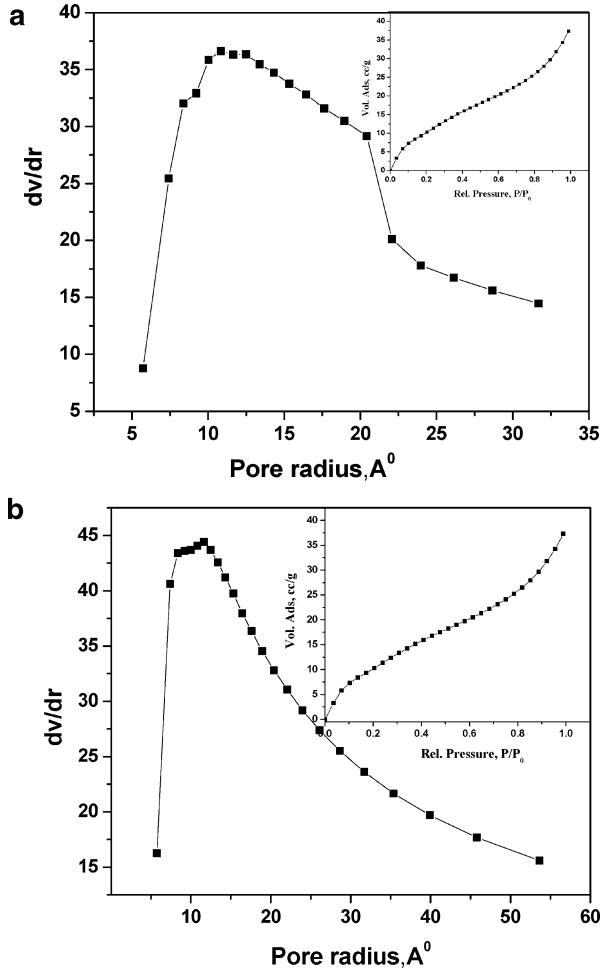

Figure 5. Pore size distribution and adsorption isotherm (inset) of cerium phosphate precursor gel after calcination at (a) 400 and (b) 800 °C.

and O−P−O bending mode of vibration, respectively.[14] The FTIR spectrum indicates that the dehydration is completed below 400 °C, and the presence of phosphate is confirmed in cerium phosphate heated at higher temperature.

Pore size distribution and surface area studies by N_2 adsorption (BET) method on cerium phosphate precursor gel after calcination at 400 and 800 °C are shown in Figure 5a and b, respectively. The presence of micropores (<2 nm) and mesopores (2−50 nm) is indicated in both the pore distribution plots in the calcined gel. Whereas a distribution of micropores with extended mesoporosity is seen in the gel calcined at 400 °C, retention of micropores and partial collapse of the mesopores are observed in the gel heated at 800 °C. The volume of mesopore decreases from 0.06641 to 0.0435 cm^3/g between the gels heated at 400 and 800 °C, respectively. Similarly, there is a reduction in surface area from 98 to 52 m^2/g when the gel is heated at 400 and 800 °C, respectively. High surface area value for the gel heated at 400 °C also explains the process of dehydroxylation and the collapse of hydrogen bonds. The BET isotherm of cerium phosphate calcined at 400 °C indicates a predominantly mesoporous nature, although at low relative pressure (P/P_o) it shows microporous character. The volume adsorbed at high relative pressure is high, indicating adsorption is in mesopores, which further transform to micropores on heating to 800 °C. For

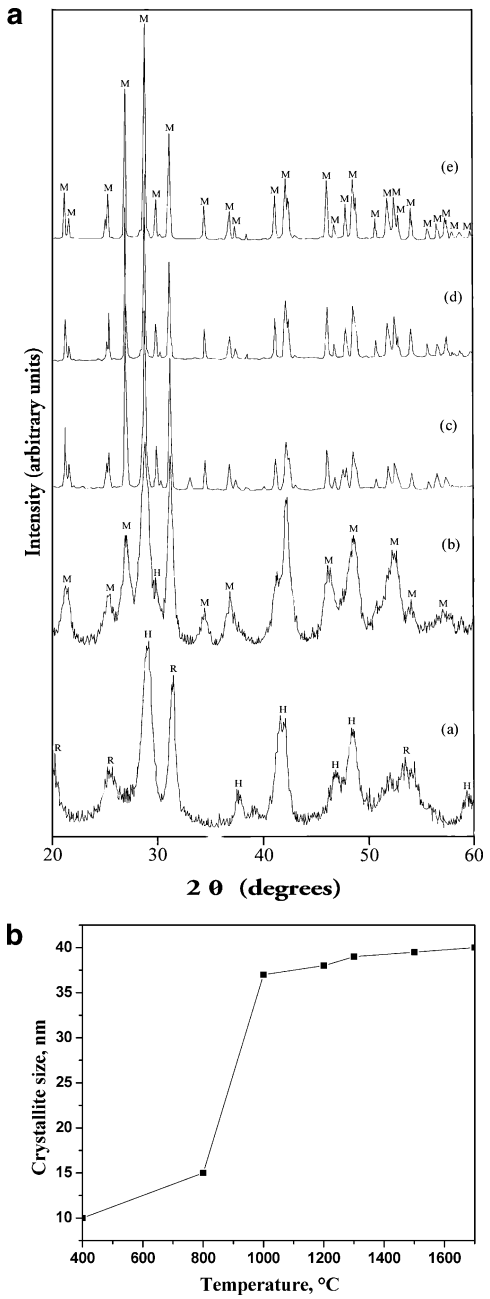

Figure 6. (a) X-ray diffraction patterns of cerium phosphate precursor gel heated at different temperatures of 400 (trace a), 800 (trace b), 1000 (trace c), 1300 (trace d), and 1700 °C (trace e); M = monazite, H = hexagonal, R = rhabdophane. (b) Plot of crystallite size versus temperature.

the vapor-phase O-alkylation of phenol over alkali Sarala Devi et al. used cerium phosphate catalysts with surface area of 6−10 m^2/g and also for oxidative dehydrogention of isobutane to isobutene Takita et al. used catalysts with surface areas of 6.8−36.6 m^2/g.[7,6] Onoda et al. reported 0.9 m^2/g of specific surface area for cerium phosphate and found that catalytic activity of rare earth phosphates was influenced significantly by specific surface area.[8] We have obtained much higher surface area than reported earlier, which may facilitate catalytic activity of the cerium phosphate in various organic reactions. The high surface area is achieved by the ultrasonicaton of the cerium phosphate sol resulting in deagglomerated nanosized cerium phosphate particles. The particle size was further calculated from BET

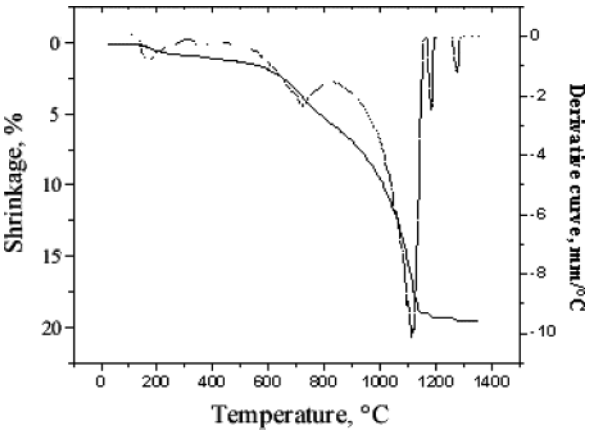

Figure 7. Dilatometric curve of cerium phosphate.

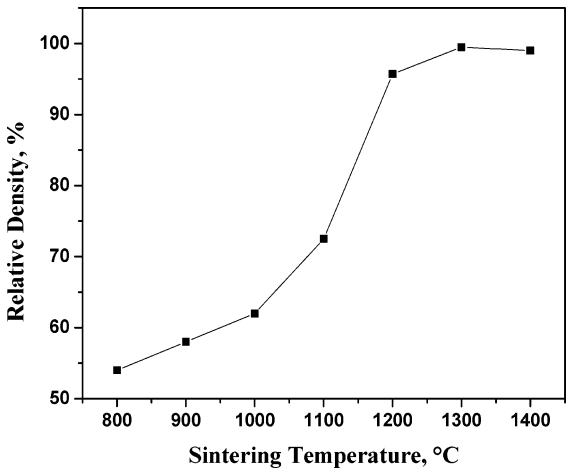

Figure 8. Plot of relative density against temperature.

surface area data using the following equation:[19]

$$D = \frac{6000}{Sd}$$

where D is average particle size (nm), S is BET surface area, and d is the density of cerium phosphate (5.22 g/cm^3). Cerium phosphates calcined at 400 and 800 °C having average particle sizes of 11 and 22 nm, respectively, were obtained.

The X-ray diffractograms of cerium phosphate precursor gel heated at different temperatures in the range of 400−1700 °C are presented in Figure 6. The gel calcined at 400 °C shows the transformation of rhabdophane (hydrated cerium phosphate) to hexagonal form. Thermal analysis supports the above observation, where the dehydration of cerium phosphate is observed below 400 °C. The major hexagonal cerium phosphate phase was identified with JCPDS file no. 4-632, and also the presence of rhabdophane (JCPDS file no. 35-0614) in the XRD pattern shows the incomplete transformation of hexagonal phase. Cerium phosphate calcined at 800 °C shows broad peaks of monazite-type monoclinic cerium phosphate (JCPDS file no. 32-0199) which became sharp above 800 °C. The crystallization of monazite-type $CePO_4$ commences above 700 °C and is in good agreement with our thermal analysis data. Earlier reports also showed that crystallization of monazite $CePO_4$ commences above 700 °C.[14] The peaks of the calcined pow-

(19) Xiong, G.; Zhi, Z.; Yang, X.; Lu, L.; Wang, X. *J. Mater. Sci. Lett.* **1997**, *16*, 1064.

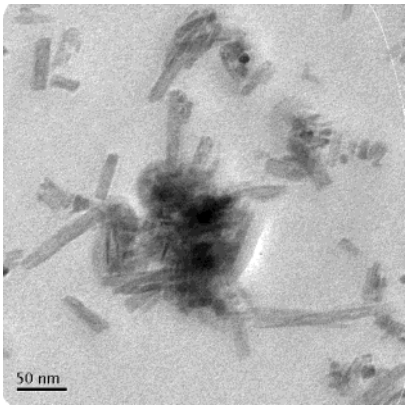

Figure 9. TEM picture of cerium phosphate precursor gel heated at 400 °C.

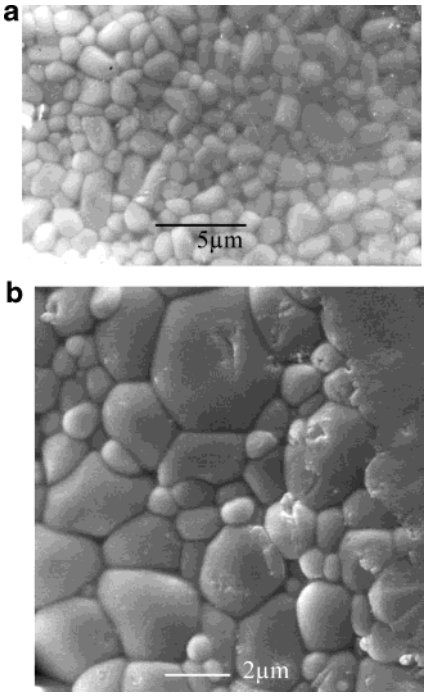

Figure 10. SEM pictures of cerium phosphate sintered at (a) 1300 and (b) 1500 °C.

ders at 1000 °C for 3 h clearly indicate that the gels were highly crystallized. The characteristic *d* values obtained exactly match the JCPDS file data. Phase stability in the temperature range up to 1700 °C was observed in the present investigation. The XRD patterns of the powders calcined at still higher temperature were similar. The crystallite size calculated from XRD patterns was in the range of ∼10 and 15 nm for lanthanum phosphate calcined at 400 and 800 °C, respectively, by using the Scherrer equation, which are comparable with that calculated from BET surface area. Figure 6b shows the plot of crystallite size versus temperature of calcination. The crystallite size increases with calcination temperature, and crystallite size 40 nm was obtained after heating to 1700 °C.

The sol−gel-derived cerium phosphate was also subjected to dilatometry for observing the sintering characteristics of the system. The nano precursor powder was calcined at 400 °C and was compacted to cylindrical pellets of 10-mm diameter and 8-mm height. The shrinkage−temperature profile measured using the dilatometer is presented in Figure 7. The densification of cerium phosphate takes place in three steps. The densification starts as early as 740 °C. This is evidenced in surface area analysis that shows the decrease in surface area of cerium phosphate calcined at 800 °C. Shrinkage of ∼5.3% was obtained between 100 and 750 °C. Fast shrinkage (∼15%) was seen in the range 800−1150 °C. A total shrinkage of about ∼25% is observed. Compared with the data from thermogravimetry and infrared spectrum, the shrinkage is due to formation of crystalline rare earth phosphate followed by densification. Relative density as high as ∼99% could be obtained by sintering at as low as 1300 °C.

The powder calcined at 400 °C was compacted, at pressure of 200 MPa, to pellets of 11-mm diam × 2-mm thickness, which were sintered in the range 800−1400 °C at a heating rate of 10 °C/min and soaked for 3 h. A relative density of ∼99% was obtained by sintering at 1300 °C. The densification features of cerium phosphate are presented in Figure 8. Earlier, Hikichi et al. reported relative density of ∼99% at 1500 °C.[9] The decrease in sintering temperature may be due to the nanosize of the $CePO_4$ particles, prepared by sol−gel route, which enhances the surface diffusion.

Transmission electron microscopic investigation of cerium phosphate precursor gel calcined at 400 °C indicates needle-like morphology of the $CePO_4$ particle which may be due to hexagonal form of $CePO_4$ derived from aqueous route at low temperature as has been reported in the literature.[13,14] An average crystallite size of 20 nm is seen in TEM presented in Figure 9. A certain agglomeration may be due to the collapse of hydrated-rhabdophane cerium phosphate particles during calcination of gel at 400 °C.

The morphology of thermally etched cerium phosphate sintered at 1300 and 1500 °C was observed under scanning electron microscope (Hitachi, 2240 Japan), and is presented in Figure 10a and b, respectively. An average grain size of ∼1 μm was noted in the sample sintered at 1300 °C and >2 μm was found for the sample sintered at 1500 °C.

Conclusions

Cerium phosphate nanoparticles were synthesized through colloidal sol−gel route involving precipitation−electrostatic stabilization and under ultrasonicated condition. A monomodal distribution with average particle size of 50 nm is obtained in precursor sol. Crystallite size is 10 nm and specific surface area is 98 m^2/g for cerium phosphate gel calcined at 400 °C. Retention of microporosity and collapse of mesoporosity are evidenced in the pore size distribution curve of cerium phosphate calcined at 800 °C. Cerium phosphate was sintered to ∼99% density at a low temperature (1300 °C). Average sintered grain size of ∼1 μm was observed. Cerium phosphate phase was stable in the temperature range investigated (400−1700 °C).

Acknowledgment. K.R. is grateful to M/s Indian Rare Earths Ltd., Mumbai, India, for providing financial support. The authors also acknowledge Dr. Tomandl and Dr. Sigrid Benfer, TU Bergakademie, Freiberg, Germany for the SEM and TEM analysis of the samples. We also acknowledge valuable discussions with Prof. P. E. D. Morgan, Rockwell Science Centre, Thousand Oaks, CA.

CM0499139